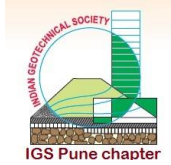


**50th
IGC****50th INDIAN GEOTECHNICAL CONFERENCE**17th – 19th DECEMBER 2015, Pune, Maharashtra, India

Venue: College of Engineering (Estd. 1854), Pune, India

ANALYSIS OF BACK-TO-BACK REINFORCED RETAINING WALLS WITH MODULAR BLOCK FACING

Sasanka Mouli S., Doctoral Student, Indian Institute of Technology Hyderabad, ce11P1006@iith.ac.in

Umashankar B., Assistant Professor, Indian Institute of Technology Hyderabad, buma@iith.ac.in

Madhav M. R., Visiting Professor, Indian Institute of Technology Hyderabad, madhavmr@gmail.com

ABSTRACT: Back-to-back reinforced retaining walls are mostly used in approach embankments for bridges and flyovers. Guidelines on the design of such walls are limited. According to FHWA codal provisions, the distance between back-to-back walls is an important parameter in estimating the lateral earth pressures on these walls. For back-to-back walls of height ' H ' with backfill angle of shearing resistance ' ϕ ', two cases are given in the code: a) the walls are sufficiently far away with the distance between the facings of reinforcements extending from the two walls (D) is greater than $H \cdot \tan(45^\circ - \phi/2)$, the walls are designed as independent walls, and b) the ends of the reinforcements for the two walls overlap by a distance more than $0.3 \cdot H$, the active lateral earth pressure is taken as zero while performing the check for external stability. If the distance between the walls is intermediate between these two cases, the lateral earth pressures of the walls are linearly interpolated. However, there is no literature available to justify the above mentioned earth pressure distribution for back-to-back reinforced walls. The objective of this study is to obtain the effect of distance between the far ends of reinforcements normalized with the wall height (D/H) on the lateral pressures at the facing of the wall and at the end of reinforcement. In this study, charts are proposed showing the variation of lateral pressures and facing displacements with depth for D/H varying from 0.0 to 0.6 and for different reinforcement stiffness ranging from 500 kN/m to 50000 kN/m.

INTRODUCTION

Mechanically stabilized earth retaining walls are the state of the art technology in place of conventional earth retaining walls. Advantages of mechanically stabilized earth walls (MSE) mainly include cost effectiveness, reduced space requirement, flexibility, and resistance to earthquake loading. Advances in materials have led to use of wide variety of reinforcement elements. The reinforcing elements can be metal strips and grids, or polymer products (e.g., geotextiles, geogrids and geomembranes).

For railroad bridge embankments or 2-to-4 lane highway bridge approach embankments, the two walls are relatively not far apart and are referred as *back-to-back* retaining walls.

Many studies are available in the literature on reinforced single retaining wall. Studies include full-scale modeling, prototype modeling, and numerical modeling evaluating the effect of different parameters. Rowe and Ho (1997) [13] studied the effects of length of reinforcement, reinforcement arrangement, number of reinforcement layers, and height of wall on the distribution of lateral pressures on the facing wall

using finite-element (FE) program. Rowe and Skinner (2001) [14] performed finite-element analysis of 8m-high, geosynthetic-reinforced wall resting on both compressible and rigid foundations, and compared the results from full-scale experiment. Ling and Leshchinsky (2003) [9] developed a numerical model to study the effects of the length, spacing and stiffness of reinforcement; the width, connection strength and interaction of the modular block; and properties of foundation and backfill soil in reinforced single retaining wall with segmental-block facing.

Wu (2007) [17] observed from the case studies that the lateral earth pressures against segmental MSE wall were much less than those obtained from Rankine's or Coulomb's earth pressure theories. Mei et al. (2009) [10] formulated a model to predict the lateral pressures for various displacements of wall, ranging from active to at-rest conditions. Different patterns of wall movement were also analyzed.

Wong (1972) [16] conducted experimental and theoretical studies to analyze back-to-back retaining walls with live loads acting on the backfill. Anchor piles were used as a retaining structure, and iron rods were used as reinforcing elements. Earth pressures due to live loads were calculated using the theory of elasticity.

Han and Leshchinsky (2010) [4] developed a numerical model in a finite-difference based software- Fast Lagrangian Analysis of Continua (FLAC)- to analyze reinforced back-to-back walls. Parametric studies were carried out by varying two parameters, *viz.*, the wall width to height ratio and the quality of backfill material, to study their effects on the required tensile strength of reinforcement, critical failure surface, and the lateral earth pressure behind the reinforced zone. The effect of connection of reinforcement in the middle was also considered.

Anubhav and Basudhar (2012) [1] studied the response of footing placed on a double-faced, wrap around reinforced walls by conducting a small-

scale laboratory tests. Authors have presented the influence of number of reinforcing layers and overlap length on load-deformation behavior, ultimate bearing pressure of footing, and initial tangent modulus of the soil. Two different multi-filament geotextiles were used in the study. Settlement of the footing and lateral deformations of wrap-around wall facing were also presented.

Katkar and Viswanadham (2012) [7] conducted centrifuge model tests to study the behavior of single vertical wall and geogrid reinforced back-to-back walls constructed using wrap-around technique. The effect of connection in the middle of the wall was also analyzed.

In working stress condition, FE analysis was done on back-to-back walls by Sherbiny et al. (2013) [15]. The effects of distance between the walls on lateral earth pressures, lateral displacements, and maximum tensions in the reinforcement were studied. Olgun and Martin II (2003) [12] modeled an overpass in FLAC, and obtained tensions within reinforcements and the lateral earth pressures on reinforced wall under seismic conditions.

Mouli and Umashankar (2014) [11] studied the effects of stiffness of reinforcement and angle of shearing resistance on the lateral pressures and lateral displacements of the facing of reinforced back-to-back walls with connected reinforcements.

PROBLEM DEFINITION

The focus of this paper is to obtain the effect of distance between the walls normalized with the wall height (W/H) on the lateral pressures at the facing of the wall and at the end of reinforcement zone. In the present study, back-to-back walls (Fig. 1) are modeled incorporating the staged construction. The effect of the stiffness of the reinforcement is also studied by varying the reinforcement stiffness from 500 kN/m to 50000 kN/m. Finite-difference-method based program FLAC is used for modeling (Itasca 2011) [6].

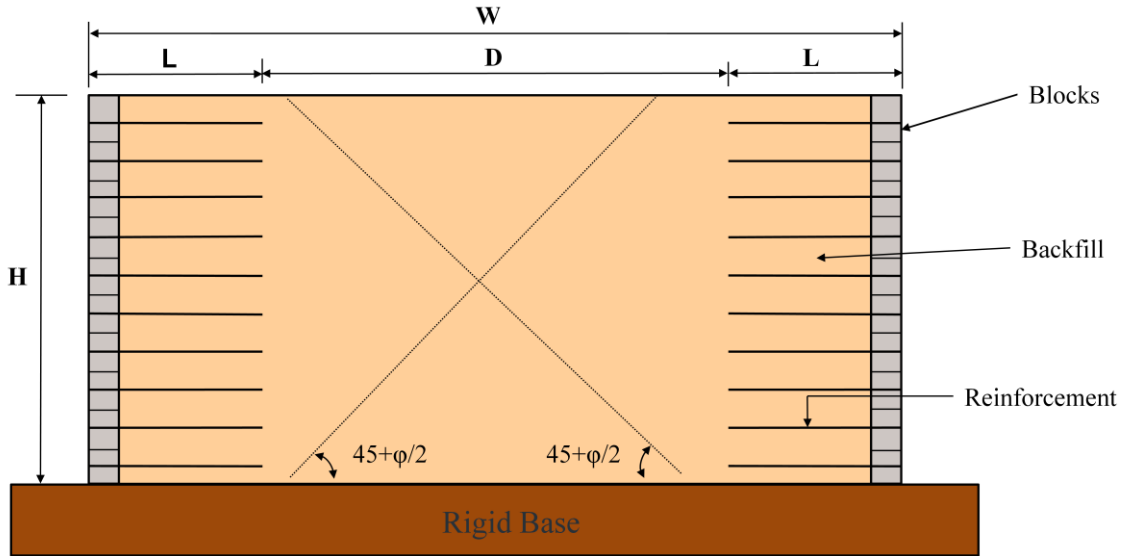


Fig. 1 Schematic of reinforced back-to-back wall

NUMERICAL MODELLING

A two-dimensional numerical model was developed using the finite-difference-method based software – Fast Lagrangian Analysis of Continua (FLAC) *version 7.00* (Itasca Consulting Group 2011) [6]. Back-to-back wall was constructed under plain-strain condition. A 6-m high wall was considered and the length of the reinforcement was fixed as 4.2m (0.7 times the wall height). The foundation soil, reinforced soil, retained soil, and facing panel were modelled as continuum.

Distance between the far ends of two reinforcements, D , was varied from 0 to $0.6H$ so that W/H ratio ranges from 1.4 to 2.0. The vertical spacing between the reinforcements was fixed as 0.6m.

Bottom of the foundation soil was fixed in both horizontal and vertical directions. Mesh convergence was done and the size of the grid was taken as approximately 0.1m. Large-strain mode was activated so that the coordinates of the grid points are updated at every step. This ensures accuracy in the numerical model, especially when high strains develop in the material.

The foundation soil was taken as rigid by giving a very high cohesion value. Reinforced and retained soils were simulated as isotropic, non-linear elastic perfectly plastic using Mohr-Coulomb failure criterion. **Table 1** gives the properties of the foundation soil, and reinforced and retained backfills.

Elastic modulus of the soil is dependent on the confining stress [2]. It is updated at every stage using the procedure adopted in Hatami and Bathurst (2005) [5]. Equation given by Duncan et al. (1980) [2] was used (Eq. (1)).

$$E_t = \left[1 - \frac{R_f(1 - \sin\phi)(\sigma_1 - \sigma_3)}{2c \cdot \cos\phi + 2\sigma_3 \cdot \sin\phi} \right]^2 \cdot K_e \cdot P_{atm} \cdot \left(\frac{\sigma_3}{P_{atm}} \right)^n \quad (1)$$

where, E_t is the tangent elastic modulus, R_f is the failure ratio, K_e is the elastic modulus number, n is the elastic modulus exponent, P_{atm} is the atmospheric pressure, ϕ is the angle of shearing resistance, c is the cohesion intercept of the soil, σ_1 is the effective vertical pressure (overburden), and σ_3 is the effective lateral confining pressure.

The wall facing was modelled as modular blocks of size 0.3 x 0.2m. Material properties of modular

blocks were assumed equal to that of concrete material (**Table 1**).

Table 1 Properties of the foundation soil, reinforced and retained backfills

Properties	Reinforced soil	Foundation soil	Modular blocks
Material type	Mohr-Coulomb	Mohr-Coulomb	Elastic
Cohesion (kPa)	0	1000	-
Angle of shearing resistance (ϕ) in deg.	34 ^o	35 ^o	-
Dilation angle in deg.	10	0	-
Shear Modulus (kPa)	3.846e4	3.846E4	8.70e6
Bulk Modulus (kPa)	8.333e4	8.332E4	9.52e6
Density (kg/m ³)	1800	1800	2400

Table 2 Constants used in the equation for stress dependent modulus of backfill soil

Properties	Reinforced soil
Elastic modulus number (K_e)	1150
Bulk modulus number (K_b)	575
Elastic modulus exponent (n)	0.5
Bulk modulus exponent (m)	0.5
Failure ratio (R_f)	0.86

Table 3 Interface properties

Properties	Block-Block interface	Block-Soil interface
Normal stiffness k_n (kPa)	11.90e6	11.90E6
Shear stiffness k_s (kPa)	10.87e6	2.31E4
Cohesion (kPa)	10	0
Friction angle (δ) (in deg.)	55 ^o	25 ^o

Table 4 Reinforcement properties

Properties	Cable element
Stiffness (J) (kN/m)	500, 5000, 50000
Poisson's ratio (ν)	0.3

Interface elements were used to simulate the interaction between the soil and the modular-block facing of the wall and between the modular blocks. In FLAC, shear strength of interface was assumed to follow Mohr-Coulomb failure criterion. Interface between the soil and block facing was simulated as frictional interface (i.e., cohesion was taken as equal to zero) and interface between the blocks was simulated as structural interface (i.e.,

both the cohesion and friction angle are present). **Table 3** provides the properties of the interfaces.

Reinforcement was simulated as cable element. Cable element in FLAC is a two-noded, one-dimensional element with high tensile stiffness and negligible compressive stiffness. The total length of the reinforcement was divided into number of segments. The number of segments was decided such that each segment of reinforcement is equal to the width of zones of the reinforced soil.

Reinforcement layers interact with soil through built-in interface properties. The interface properties were inputted in FLAC in terms of grout material properties. Fig. 2 shows the reinforcement that was rigidly connected to the wall facing by fixing the left end of the cable element to nodes of the wall facing to simulate the rigid connection existing in the field [8]. **Table 4** provides the reinforcement properties.

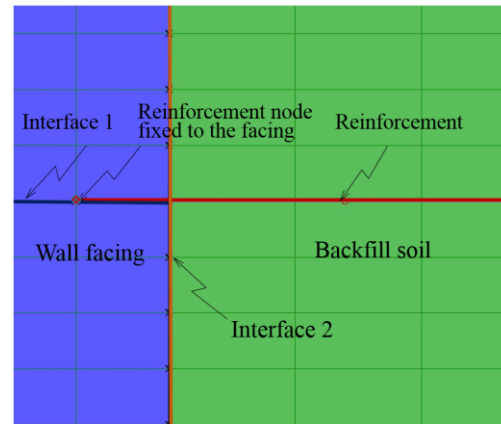


Fig. 2 Structural node fixed rigidly to the facing panel

The model wall was constructed in stages. Every lift of soil was of 0.3m height. After the soil layer was placed, the model was solved for equilibrium. The elastic modulus was then updated using Eq. (1) and **Table 2**, and again solved for equilibrium. The next layer of soil was now placed on the deformed grid of the previous layer. At every stage, the equilibrium ratio was maintained to be less than 1e-3. Equilibrium ratio is the largest ratio of maximum unbalanced force to the applied force considered at every grid point.

RESULTS AND DISCUSSION

Design charts were developed showing the variation of normalized lateral pressures at the facing of the wall and at the far end of reinforcement zone with the normalized depth of the wall. The lateral pressures were normalized with the product of unit weight of soil and total height of the wall ($\gamma \cdot H$) (Eqs. 2 & 3) and the depth of the wall was normalized by the height of the wall (H) (Eq. 4).

$$\sigma_{hr}^* = \frac{\sigma_{hr}}{\gamma H} \quad (2)$$

$$\sigma_{hf}^* = \frac{\sigma_{hf}}{\gamma H} \quad (3)$$

$$Z^* = \frac{Z}{H} \quad (4)$$

where, σ_{hr}^* and σ_{hf}^* are the normalized lateral earth pressures at the far end of reinforced zone and at the facing; σ_{hr} and σ_{hf} are the lateral earth pressures at the far end of reinforced zone and at the facing, Z^* is the normalized depth of the wall, Z is the depth of the wall from the top, H is the height of the wall, and γ is the unit weight of the soil.

Parametric study was done for different stiffness of the reinforcement. Stiffness value of reinforcement was varied from 500 kN/m to 50000 kN/m. Graphs were plotted between normalized lateral earth pressure and normalized depth of wall. Results from FLAC program were fitted with linear trend lines using Matlab program as shown in Fig. 3 (a) and (b).

Lateral Earth Pressures at the end of reinforced zone

Distribution of lateral earth pressures at the far end of the reinforced zone is essential in the analysis for external stability. The variation of normalized lateral pressures at the end of reinforcement zone (i.e. at the distance of 4.2m from the facing of the wall in this case) with the normalized depth was

provided for various W/H ratios and for different stiffness values.

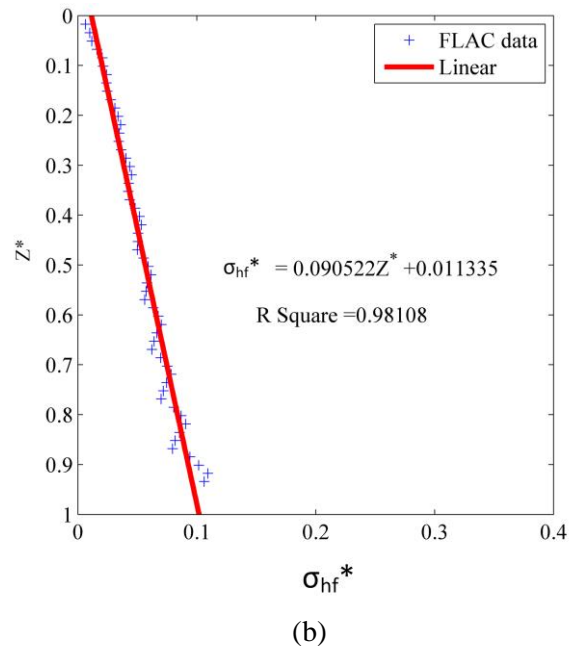
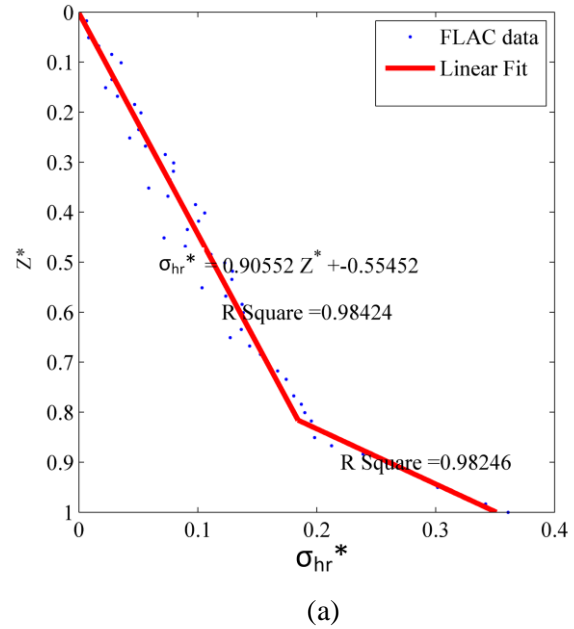


Fig. 3 Fitted plots for normalized lateral earth pressures from FLAC for the case- W/H=2.0 and J=5000 kN/m: (a) at the far end of reinforcement zone, and (b) at the facing

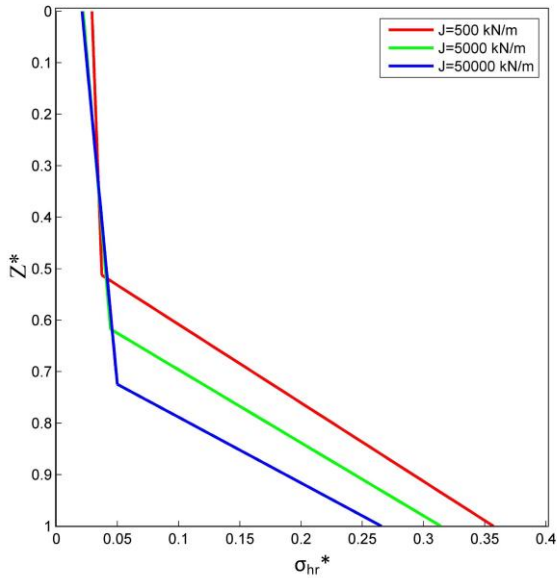


Fig. 4 Fitted variation for lateral pressures at the end of reinforcement zone for $W/H=1.4$

It was observed that the normalized pressures at the end of reinforcement zone follow a bilinear pattern for all the W/H ratios. A critical depth, Z_c , was proposed at which the slope of the lateral earth pressure profile changes with respect to the depth of the wall. In the case of $W/H=1.4$ (Fig. 4), critical depths for the reinforcement stiffness values equal to 500 kN/m, 5000kN/m, and 50000kN/m were found to be equal to $0.5H$, $0.63H$ and $0.73H$ from the top of the wall. The normalized lateral earth pressures within the critical depth were almost constant and equal to $0.05\gamma H$ for all the values of reinforcement stiffness considered in the study. Beyond critical depth, the lateral earth pressures were found to vary significantly with the reinforcement stiffness. Lateral pressures corresponding to 50000 kN/m stiffness value were lower than that of the stiffness values of 500kN/m and 5000 kN/m. The lateral pressures were higher than that of the active earth pressures at the bottom of the wall. This might be due to friction mobilized between the backfill soil and foundation soil was higher. From the results, it can be observed that the influence of one wall on the other increases as the stiffness of the reinforcement decreases. The results were found to compare well with the lateral pressure plots presented in Han and Leshchinsky (2010) [4]. Results obtained from the study contradicted the code in the assumption of linear

interpretation between active condition and zero lateral earth pressures.

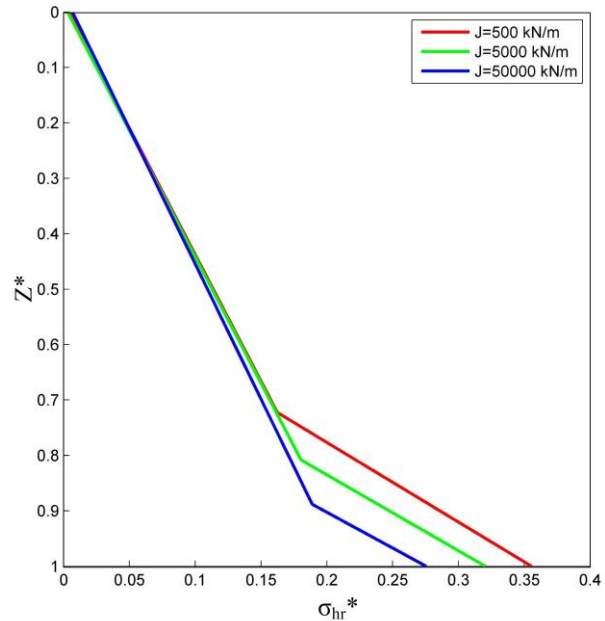


Fig. 5 Fitted variation for lateral pressures at the end of reinforcement zone for $W/H=1.7$

In the case of $W/H=1.7$ (Fig. 5), the slopes of the lines were 5.0 for all three reinforcement stiffness values which were lower than that of $W/H =1.4$. But the depths of Z_c value for different reinforcement stiffness values were slightly higher than that of $W/H=1.4$. The slopes of the fitted variation decreased a little when the W/H ratio is increased to 2.0 (Fig. 6). Insignificant increase in the Z_c was observed for $W/H=2.0$ case from that of $W/H=1.7$ case. Fig. 7 shows the variation of Z_c with W/H ratio.

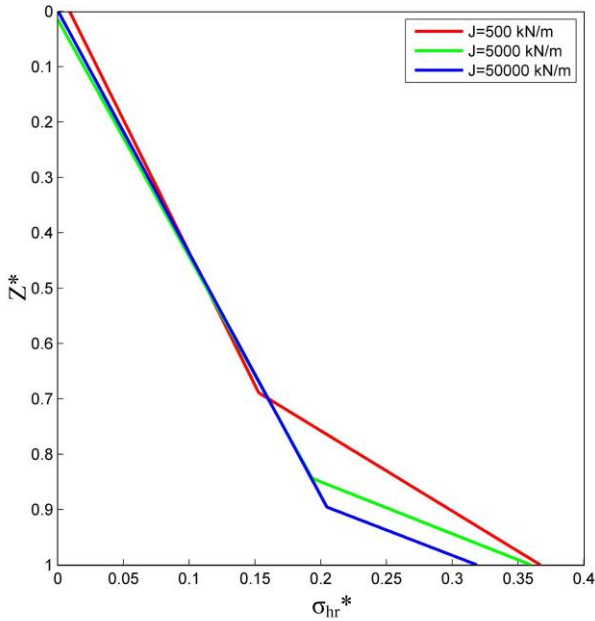


Fig. 6 Fitted variation for lateral pressures at the end of reinforcement zone for $W/H=2.0$

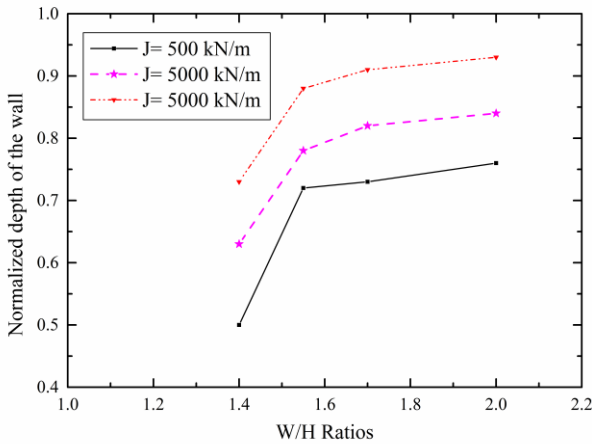


Fig. 7 Variation of Z_c with W/H ratio for various reinforcement stiffness values

Lateral pressures at the facing normalized with respect to H

The lateral pressures at the facing are also of great significance in the internal stability analysis. When $W/H = 1.4$ (Fig. 8), critical depth of the wall (Z_c) was equal to $0.9H$ from the top of the wall for all three reinforcement stiffness values considered in the study.

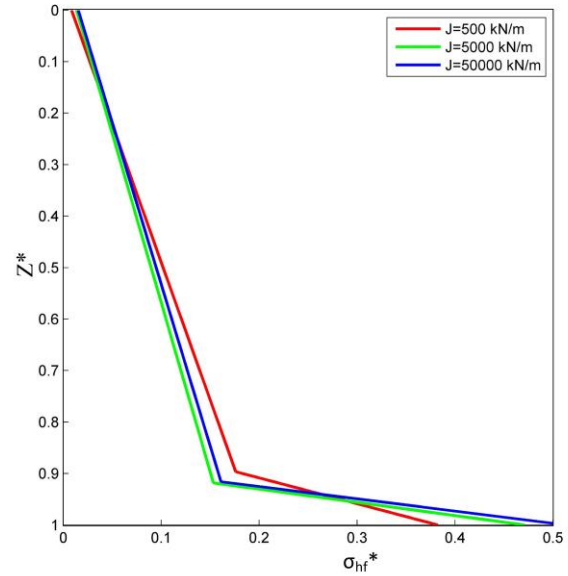


Fig. 8 Fitted variation for lateral pressures at the wall facing for $W/H=1.4$

The rate of increase in lateral earth pressure with depth increases as the stiffness of reinforcement decreases. This implies that at a given depth, lateral pressures reduce with increase in the reinforcement stiffness. High lateral pressures were observed at the bottom of the wall which may be due to constrained movement at the bottom.

When the W/H ratio was increased to 1.7 (Fig. 9), the lateral earth pressures at the facing for reinforcement stiffness value of 5000 kN/m and 50000 kN/m were equal for W/H ratio=1.55 and 1.7. In the case of $W/H = 2.0$ (Fig. 10), the critical depth vanishes and a significant reduction in lateral earth pressures were observed when the reinforcement stiffness increases from 500kN/m and 5000 kN/m. However, the effect of reinforcement stiffness on the lateral earth pressures was negligible for stiffness higher than 5000 kN/m.

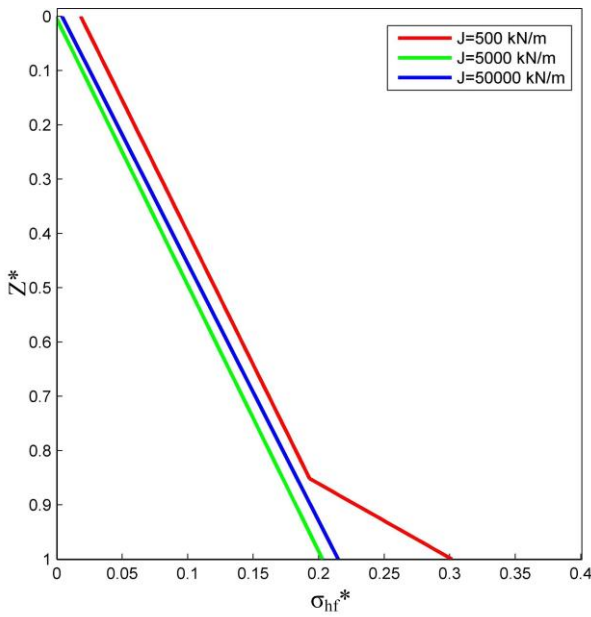


Fig. 9 Fitted variation lateral pressures at the wall facing for W/H=1.7

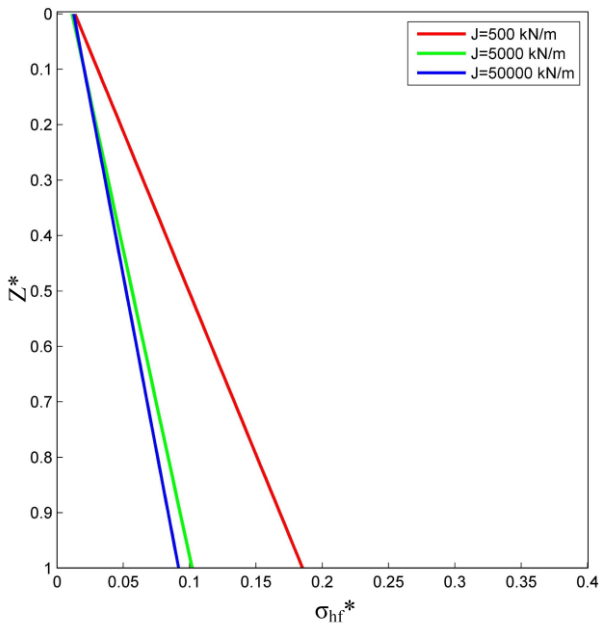


Fig. 10 Fitted variation for lateral pressures at the wall facing for W/H=2.0

CONCLUSIONS

The lateral pressures at the end of reinforcement zone and at the wall facing for various W/H ratios in back-to-back walls were analyzed. Following conclusions can be made:

- Lateral earth pressures at the end of reinforcement zone followed a bilinear pattern for all the W/H ratios. Magnitude of lateral earth pressures increased as the W/H was increased, but was found to be much less than that of the active earth pressures. However, the earth pressures at the bottom of the wall were higher than the active condition and were constant for all W/H ratios.
- Critical depth Z_c was proposed for various W/H ratios and for various stiffness values to predict the lateral pressures at the end of reinforcement zone. The value of Z_c had increased significantly as W/H increases from 1.4 to 1.55. Further, much change was not observed when the W/H ratio was increased from 1.55 to 2.0.
- Charts were proposed showing the variation of normalized lateral pressures at the facing with normalized depth. The variation was found to be bilinear for lower W/H ratios. However, for higher W/H, the variation was linear. Reinforcements with higher stiffness changes to linear pattern at lower W/H ratio than that of reinforcements with lower stiffness values.
- A significant reduction in lateral earth pressures at the facing was observed when the stiffness of the reinforcement was increased from 500 kN/m to 5000 kN/m. However, further increase in the stiffness from 5000 kN/m to 50000 kN/m, the increase in lateral earth pressures were found to be insignificant.

REFERENCES

- Anubhav and Basudhar, P.K. (2012), Footing on double-faced wrap-around reinforced soil walls, *Ground Improvement*, 167(G12), 73-87.
- Duncan, J.M., Byrne, P., Wong, K.S. and Mabry, P. (1980), Strength, stress-strain and bulk modulus parameters for finite element analysis of stresses and movements in soil masses, Dept. of Civil Engg., University of California, Berkeley, Calif. *Report No. UCB/GT/80-01*.

3. Elias, V., Christopher, B.R. and Berg, R.R., (2001), Mechanically stabilized earth walls and reinforced soil slopes design and construction guidelines, *Publication No. FHWA-NHI-00-043*.
4. Han, J. and Leshchinsky, D. (2010), Analysis of back to back mechanically stabilized earth walls, *J. of Geotext. and Geomem.*, 28, 262–267.
5. Hatami, K. and Bathurst, R.J. (2005), Development and verification of a numerical model for the analysis of geosynthetic-reinforced soil segmental walls under working stress conditions, *Can. Geotech. J.* 42, 1066–1085.
6. Itasca (2011), FLAC -Fast Lagrangian Analysis of Continua Version 7.00., *Itasca Consulting Group Inc., Minneapolis, Minn.*
7. Katkar, B.H. and Viswanadham, B.V.S. (2012), Centrifuge Studies on the behavior of back-to-back geogrid reinforced soil walls, *Proc. of the 1st Asian Workshop on Phy. Modelling in Geot.*, Nov 14-16, Bombay, B.V.S. Viswanadham (eds.), 337-349.
8. Lee, W.F. (2000), *Internal stability analyses of geosynthetic reinforced retaining walls*, Ph.D. Dissertation, University of Washington, USA.
9. Ling, H.I. and Leshchinsky, D. (2003), Finite element parametric study of the behavior of segmental block reinforced-soil retaining walls, *Geosynthetic Intl.*, 10(3), 77-94.
10. Mei, G., Chen Q. and Song, L. (2009), Model for predicting displacement dependent lateral earth pressure, *Can. Geotech. J.*, 45, 969-975.
11. Mouli, S.S. and Umashankar, B. (2014), Numerical analysis of MSE walls considering wall friction and reinforcement stiffness, *Proc. of 14th IACMAG*, Sep 22-25, Kyoto, Japan, F.Oka, A.Murakami, R.Uzuoka, S.Kimono (eds.), Balkema (Pbs.), 1119-1123.
12. Olgun, C.G. and Martin II, J.R. (2003), Performance and analysis of Arifiye over pass reinforced earth walls during the 1999 Kocaeli (Turkey) earthquake, *Reinf. Soil Engg. Adva. In Resrch. and Pract.*, H.I.Ling, D.Leshchinsky and F.Tatsuoka (Eds.), Ch-22
13. Rowe, R.K. and Ho, S.K. (1997), Continuous panel reinforced soil walls on rigid foundations, *J. of Geot. and Geoenv. Engg.*, 123(10), 912-920.
14. Rowe, R.K. and Skinner, G.D. (2001), Numerical analysis of geo-synthetic reinforced retaining wall constructed on a layered soil foundation, *J. of Geotext. and Geomem.*, 19, 387- 412.
15. Sherbiny, R.E., Ibrahim, E. and Salem, A. (2013), Stability of back-to-back mechanically stabilized earth walls, *Geo-congress, Mar 3-7, San Diego, California*, M.A. Pando, D.Pradel, C.Meehan and J.F.Labuz (eds.) ASCE (Pbs.) 555-565.
16. Wong, W.W. (1972), *Theoretical and experimental study of a tied back to back retaining wall for railway loading*, Master of Engineering, Thesis Report, Sir George Williams University, Montreal, Canada.
17. Wu, J. (2007), Lateral earth pressure against the facing of segmental GRS walls, *Geosyn. In Reinf. And Hydr. Appli.*, 1-11.